

Table S1. Summary of physicochemical properties of ZnO NPs

Parameter	Value
Particle size (nm) ^a	<50
TEM particle size ^a	44 ±6
Particle density (g/cm ³)	5.60
BET specific surface area measured (m ² /g)	11.2
Hamaker constant (J) in water ^b	1.9×10 ⁻²⁰
Zero-point charge (pH _{zpc}) (See figure S1B)	9.2
Zeta potential (mV) in pure water	+20
Net energy barrier (KT) ^c in pure water	45.1
Aggregation coefficient (S, dimensionless)	280
Moisture content by TGA (wt. %) ^a	1.9
Purity by ICP-OES (wt.%)	96.96 %

^a Vendor reported

^b [1]

^c 1 KT=4.1142×10⁻²¹ J at 25 °C

ICP-OES: Inductively Coupled Plasma Optical Emission Spectroscopy

1. Materials and methods

1.1. Sample preparation and collection

The industrial wastewater was collected from the of wastewater treatment plant and stored in 5L amber reagent bottle to avoid light. The synthetic sea water, groundwater, fresh water media and domestic wastewaters were prepared in the nano-pure water according to previously described methods [2–5]. All salts used were ACS reagent grade and purchased from local suppliers. Prior to use all waters were filtered through 0.45µm glass fiber filter and stored in dark at 4 °C.

Table S2. Natural and synthetic water characteristics

Parameter	Unit	Tap water	Industrial Wastewater	Domestic Wastewater	Freshwater	Groundwater	Seawater
pH ^a	-	7.02	7.56	7.81	6.90	7.51	7.90
Conductivity ^a	us/cm	82.42	619	2280	119	965	26100
IS	mM/L	0.002	8.90	34.0	0.79	12.09	381
TOC	mg/L	ND	35	25	6	0	5.51
HCO ₃	mg CaCO ₃ /L	>80	-	56	12	153	60
PO ₄	mg/L	-	ND	2.71	0.64	0	0
Na ⁺	mg/L	0.31	15.0	325.3	0	158	6350
K ⁺	mg/L	0.06	7.53	38.59	1.20	8.59	230
Cu	mg/L	-	0.39	0.08	0	0	0
Fe	mg/L	-	ND	0.35	0	0	0
Mg ²⁺	mg/L	0.14	27.1	77.0	3.49	27.40	815
As	mg/L	-	68.52	0	0	0	0
Ca ²⁺	mg/L	0.81	16.11	119.90	1.50	49.50	245
Cl ⁻	mg/L	0.28	22.40	501	6.61	141	10500
SO ₄ ²⁻	mg/L	-	10.52	310	0	20	950
Sb	mg/L	-	58.77	0	0	0	0

-: Not Measured

ND= Not detected

^a Measured in lab

1.2. Determination of the absorption wavelength and concentration

The ZnO NPs absorption spectra were measured using UV-Vis spectrometer (Optizen, 2120 UV-Vis, Mecasys, Korea). The absorption of ultra violet (UV) light by ZnO NPs within specific concentration range can fit the Beer-Lambert law, so the change in the absorbance may directly reflect concentration of ZnO NPs [6]. The solution was placed in a 1cm pathway of high-grade UV quartz cuvette in order to minimize the scattering effect. The concentration range of this study can be regarded as a single scattering event because the scattering mean-path is much greater than the pathway of the cuvette. The scattering cross-section of ZnO NPs was small compared with the absorption cross-section and can be neglected.

As shown in the full wavelength scanning data, the spectrum of 100 mg/L ZnO NP is characterized by a strong absorption in an UV band extending considerably into the UV-range, with absorption peak at wavelength of 370 nm (Figure S1A). In order to determine the concentration of the ZnO NP in sample, we measured the ratio emitted to absorbed intensities, respectively. The absorbed intensity is determined in terms of absorbance by using the Beer-Lambert law:

$$A = -\log_{10}\left(\frac{I}{I_0}\right) = (\log_{10e})\epsilon l C_M \quad (1)$$

where A is the measured absorbance, I_0 and I are incident and transmitted intensities, ϵ [$\text{cm}^{-1}\cdot\text{M}^{-1}$] is the molar absorptivity of the sample, l is the pathway length, and C_M [mole /L] is the molar concentration. Following this approach, a standard curve (Figure S2B) was used as the quantitative criterion of ZnO NPs concentration.

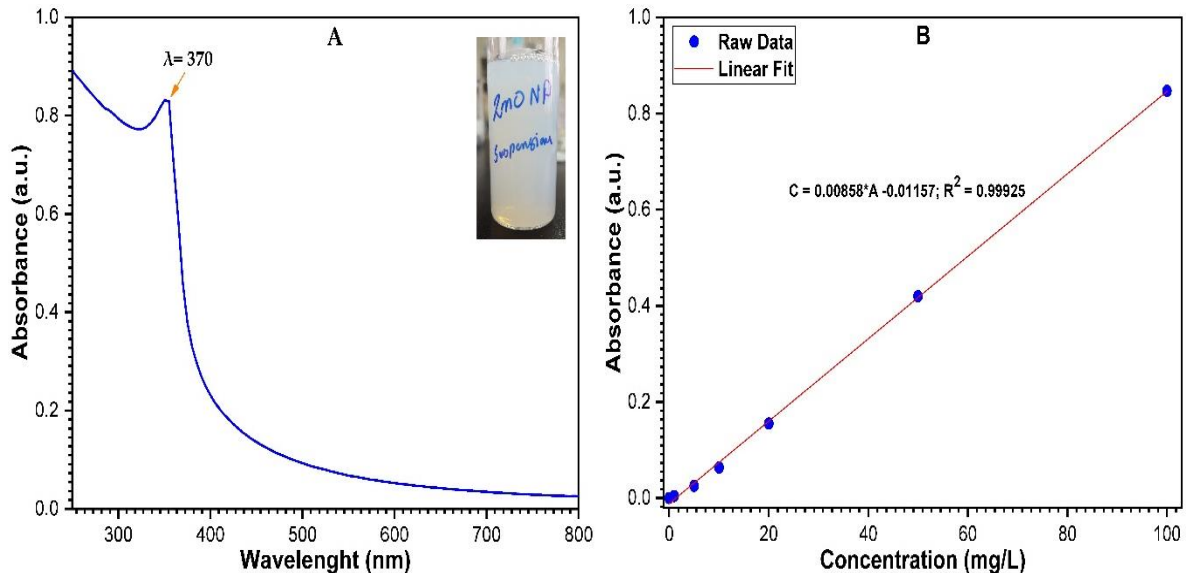


Figure S1. (A) UV-Vis spectra of ZnO NP (100mg/L) in pure water by full wave scanning; (B) Standard calibration curve of ZnO NPs concentration.

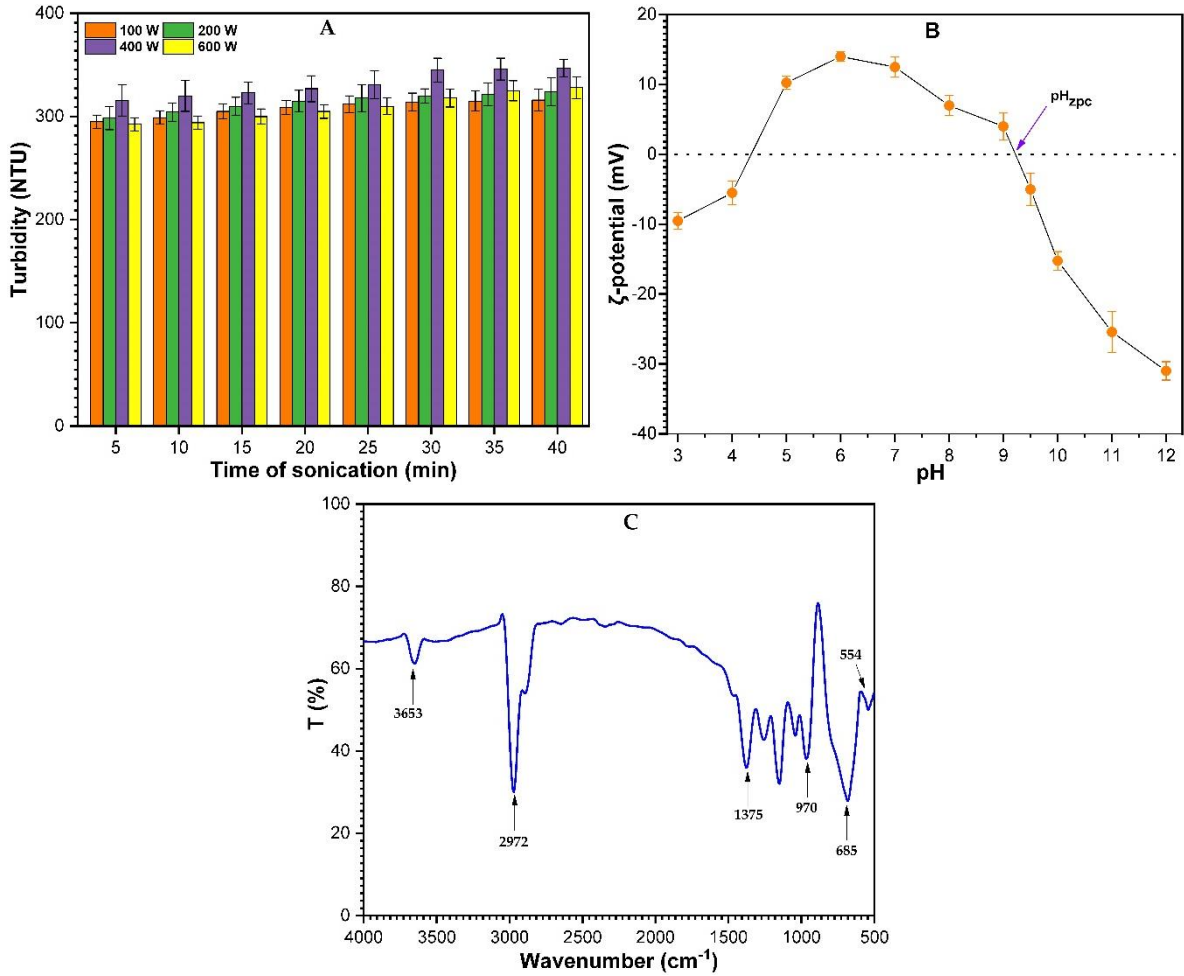


Figure S2. (A)Effect of ultrasonic time (5 - 40 min) and ultrasonic power (100 - 600 W) on suspension stability of ZnO NPs (100 mg/L); (B) Zeta potential of ZnO NPs suspension (mean± SD, n=3) at different pH; (C) FTIR spectrum of ZnO NPs used in this study.

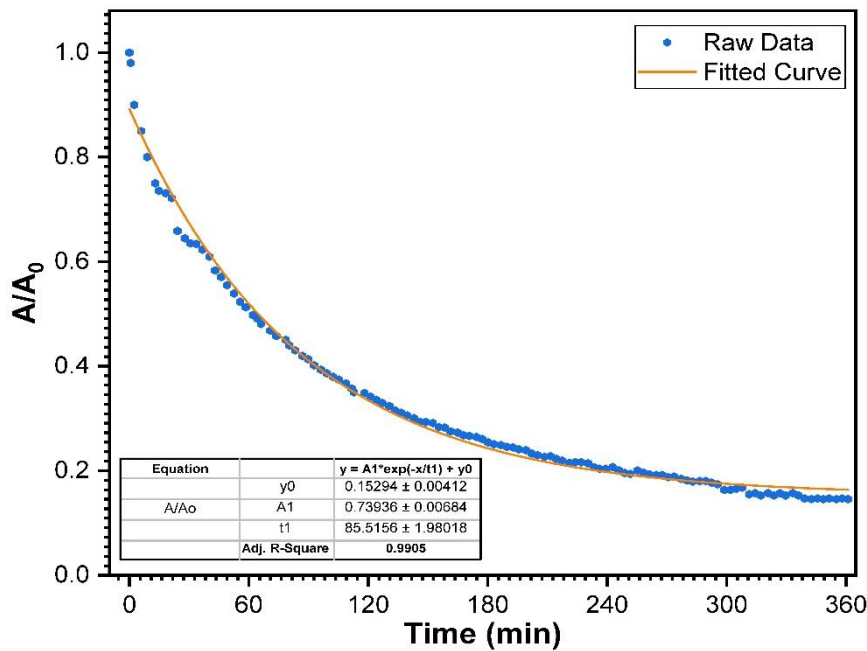


Figure S3. Fit of the sedimentation data to the stokes equation. Exponential model for 100 mg/L, 50nm ZnO NPs at pH 9 in pure water.

Table S3. Settling velocity and viscosity of ZnO NPs suspension at various temperature

Temperature (°C)	Viscosity (N.s/m ²)	Settling velocity (cm/hour)
15	1.139 × 10 ⁻³	1.978 × 10 ⁻³
25	0.890 × 10 ⁻³	2.533 × 10 ⁻³
35	0.726 × 10 ⁻³	3.105 × 10 ⁻³

1.3. Taguchi orthogonal array (OA) Matrix Design and Analysis

The traditional fractional factorial matrix design method originally developed by Fisher have been widely used in field of science and engineering [1]. However, this method might be subjected to their complexities and requirement for a large number of experiments to be carried out as the number of the designed parameters increased. While Taguchi orthogonal array (OA) matrix design is considered powerful tool that provides a simple, efficient and systematic approach to identify significant factors under designated ranges of all selected parameters. The method is valuable when the designed parameters are qualitative and discrete. In recent years, the Taguchi experimental design has been used in many industries to optimize the operating conditions for the waste water treatment and air pollution control [7,8]. ANOVA table 5. consist if sum of squares (SS), mean squares (MS), degree of freedom (DOF), percent contribution (%) and F- ratio of sum of squares to mean square of the experimental error. The Experimental error was calculated from the three designated empty columns and sum of square of error. While in the design of experiment (DOE) the F-ratio can be used for qualitative understanding of the relative factors effects. A very large F-ratio corresponded to the effect of give factor is large compared to the error variance. Therefore, the larger value of the F-ratio, the more important the given factor influencing the process response. In this analysis the Percentage contribution of each environmental parameter and each interaction was also determined.

References

1. Ackler, H. D.; French, R. H.; Chiang, Y. M. Comparisons of Hamaker constants for ceramic systems with intervening vacuum or water: From force laws and physical properties. *J. Colloid Interface Sci.* **1996**, *179*, 460–469, doi:10.1006/jcis.1996.0238.
2. Dickson, A. G. Thermodynamics of the dissociation of boric acid in synthetic seawater from 273.15 to 318.15 K. *Deep Sea Res. Part A. Oceanogr. Res. Pap.* **1990**, *37*, 755–766, doi:https://doi.org/10.1016/0198-0149(90)90004-F.
3. Marine Biological Laboratory (Woods Hole, M. .; Cavanaugh, G. M. *Formulae and methods IV [i.e., 4th ed.] of the Marine Biological Laboratory Chemical Room.*; Woods Hole, Mass., 1956;
4. Schnabel, W. E.; Dietz, A. C.; Burken, J. G.; Schnoor, J. L.; Alvarez, P. J. Uptake and transformation of trichloroethylene by edible garden plants. *Water Res.* **1997**, *31*, 816–824, doi:10.1016/S0043-1354(96)00303-X.
5. USEPA, U. S. Environmental Protection Agency (2002) Methods for measuring the acute toxicity of effluents and receiving waters to freshwater and marine organisms; EPA-821-R-02-012.
6. Kristiansson, O.; Lindgren, J.; De Villepin, J. A quantitative infrared spectroscopic method for the study of the hydration of ions in aqueous solutions. *J. Phys. Chem.* **1988**, *92*, 2680–2685, doi:10.1021/j100320a055.
7. Chyang, C.-S.; Wu, K.-T.; Lin, C.-S. Emission of nitrogen oxides in a vortexing fluidized bed combustor. *Fuel* **2007**, *86*, 234–243, doi:https://doi.org/10.1016/j.fuel.2006.06.013.
8. CBC, R.; HL, Q. Advanced oxidation processes for wastewater treatment: Optimization of UV/H₂O₂ process through a statistical technique. *Chem. Eng. Sci.* **2005**, *60*, 5305–5311, doi:10.1016/j.ces.2005.03.065.